

RAL 94011  
COPY 2 RAL-94-011  
Accn: 221775  
RAL-94-011

Science and Engineering Research Council

# Rutherford Appleton Laboratory

Chilton DIDCOT Oxon OX11 0QX

RAL-94-011

## The Chilbolton Advanced Meteorological Radar: a Tool for Multi-Disciplinary Atmospheric Research

M Thurai J D Eastment K L Morgan and J W F Goddard

February 1994

**Science and Engineering Research Council**

**"The Science and Engineering Research Council does not accept any responsibility for loss or damage arising from the use of information contained in any of its reports or in any communication about its tests or investigations"**

# **The Chilbolton Advanced Meteorological Radar ( a tool for multi-disciplinary atmospheric research )**

by

M. Thurai, J. D. Eastment, K.L. Morgan and J.W.F. Goddard

Radio Communications Research Unit  
Rutherford Appleton Laboratory  
Chilton, Didcot, Oxon OX11 0QX, UK

---

## **1. Introduction**

It is now over 20 years since the first ex-air surveillance S-band radar was installed on the 25 metre antenna at Chilbolton, near Winchester, for studies of the effects of rain on communications systems. Since that time, continuing advances in technology in areas as diverse as microwave components and digital signal processing hardware have seen a steady development in the functionality of the radar, keeping it at the forefront of meteorological research radars throughout the world. Today, the radar is used not only for propagation studies, but for cloud physics, hydrology, meteorology, and environment related programmes. We describe here recent developments, which include the implementation of polarisation-diversity techniques as well as added phase and Doppler capabilities. Section 2 deals with the reasons for developing the switched polarisation method, whilst section 3 deals with its hardware realisation. Some aspects of the theory behind the signal processing are considered in section 4, together with their software implementation and a brief description of the overall system. Finally, section 5 outlines the parameters measured by the Chilbolton Radar and gives examples of areas where the data are currently being used.

## **2. Rainfall rates and microwave attenuation derived from radar**

### 2.1 Reflectivity-Rainfall Rate Relationships

The most frequent requirement of a meteorological radar is to estimate rainfall rate, hence much of the initial work in radar meteorology was aimed at optimising the relation between the power scattered back from rain (the reflectivity,  $Z$ ), and the rainfall rate,  $R$ , as measured by,

for example, a rain gauge on the ground. For communications system designers, the equivalent parameter is the microwave attenuation due to rain. Over 300 different relationships between Z and R have been published since this work began, but the lack of a unique solution is not too surprising when it is realised that Z depends on the sixth power of the rain drop diameter, whereas rainfall rate (and microwave attenuation) is roughly proportional to the third power (i.e. the volume of water).

It is common experience that drop sizes can vary considerably, e.g. rain can consist of mainly very small drops (drizzle), or very large drops (in the early stages of a thunderstorm) with a wide range in between. Because of the drop size dependence, reflectivity measured for a few large drops, which would cause a low rainfall rate and little microwave attenuation, could equal the reflectivity measured for many small drops, which would cause a high rainfall rate, and significant attenuation.

## 2.2 Differential Reflectivity

Various techniques have been explored to overcome this ambiguity. Without doubt, the most successful to date has been that employing fast polarisation switching. The first implementation of this technique, originally proposed by Seliga and Bringi<sup>1</sup> at Ohio State University in the US, was made on the Chilbolton 3 GHz radar in 1978 (see figure 1). Due to the effects of gravity, air resistance and surface tension, raindrops take up an oblate spheroidal shape as they fall, back scattering a larger power from a horizontally polarised incident wave than a vertically polarised one. Moreover, the degree of oblateness is directly proportional to the size of the drops, as shown in figure 2, where it can be seen that small raindrops are virtually spherical, whilst larger drops are quite oblate. Of course, a radar does not measure the back scattered power from just one raindrop; the volume illuminated by a single pulse contains many thousands of drops, with a range of sizes, called the *drop size distribution (DSD)*. The polarisation difference, or *differential reflectivity*,  $Z_{dr}$ , is defined as:

$$Z_{dr} = 10 \log_{10}(Z_H/Z_V) \quad [1]$$

where  $Z_H$  and  $Z_V$  are the horizontally and vertically polarised returns, respectively, from the ensemble of rain drops in the radar pulse volume. As mentioned in section 2.1, the relative numbers of differently sized drops varies from one type of rain to another, but measurements of drop sizes show that, on average, the distribution is exponential, i.e.

$$N(D)dD = N_0 e^{-\frac{3.67 D}{D_0}} dD \quad [2]$$



**Figure 1 : The Chilbolton 3 GHz radar**

where  $N(D)dD$  is the number of drops in the size range  $D$  to  $D+dD$ ,  $N_0$  is a constant and  $D_0$  is the *median* drop size of the DSD. There is a direct relationship between  $D_0$  and the differential reflectivity, as shown in figure 3. Thus we can obtain the  $D_0$  value from the measured  $Z_{dr}$  for a given volume of rain, and then the reflectivity measurement yields the value of  $N_0$ . With the DSD completely characterised, it is straightforward to obtain the rainfall rate, or the microwave attenuation for any frequency up to at least 30 GHz.

However, the usefulness of the differential reflectivity parameter does not stop here. As is often the case with novel measurements, a somewhat unexpected additional benefit was obtained, due to the sensitivity of the  $Z_{dr}$  signature to the differing dielectric properties of ice and water. In contrast to raindrops, dry ice particles exhibit a much reduced polarisation difference for a similar shape. Thus many forms of ice, such as needles, snowflakes and hail exhibit only a small  $Z_{dr}$  signature, until they begin to melt. But as this process begins, they show the combined effect of quite asymmetrical shapes together with increased dielectric constant. A pronounced increase in  $Z_{dr}$  is the result, and the phase of the hydrometeors can be inferred<sup>2,3</sup>.

The oblateness of raindrops also causes another phenomenon, namely the differential propagation phase shift between horizontally and vertically polarised signals (see Figure 4). There are in fact two components to the measured phase of the return signal, *viz.* the propagation phase and the back scatter phase. At 3 GHz, the difference in the back scatter phase between the two orthogonal polarisations can be neglected (at least for rain), hence only the propagation phase contributes. Since this is a measure of the cumulative effect of propagation between the radar and the target volume, parameters such as average rainfall rate or integrated path attenuation caused by the intervening medium can be directly estimated. Differential phase measurements can also provide a useful means of identifying the melting regions as well as estimating water content in the ice region. Very recently, it has been shown that it provides an accurate technique to calibrate weather radars<sup>4</sup>, a critically important issue that concerns all radar meteorologists.

### **3. Radar Hardware**

The actual implementation of the  $Z_{dr}$  technique is not straightforward, due to the rapidly fluctuating echoes from successive radar pulses as large numbers of raindrops reshuffle their positions (see section 4.1). Very rapid switching is required, faster than the  $\approx 10$  milliseconds decorrelation time of the rain echoes, and, in the case of the Chilbolton radar, the peak powers that must be switched are of the order of 600 kW. It was decided at a very early stage of the design that in order to switch these large powers and retain a stability between polarisations of

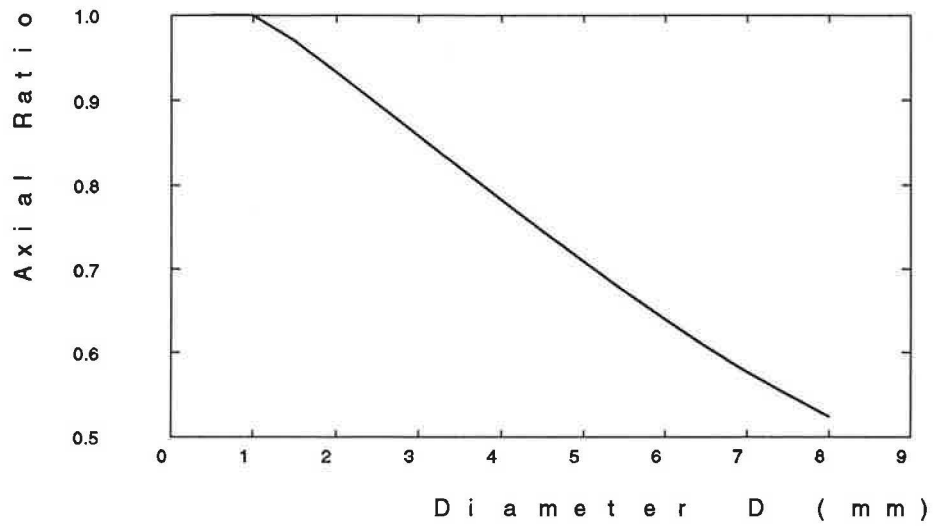


Figure 2: Variation of the ratio of the minor to major axes of rain drops with drop diameter.

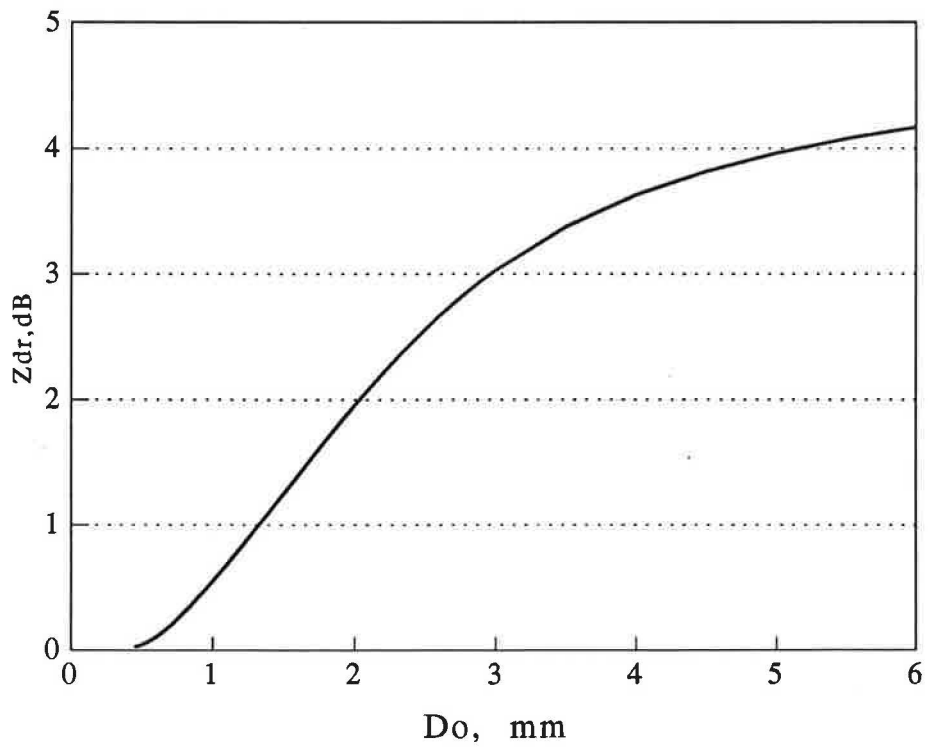


Figure 3: Relationship between  $Z_{DR}$  and  $D_o$  for an exponential drop size distribution

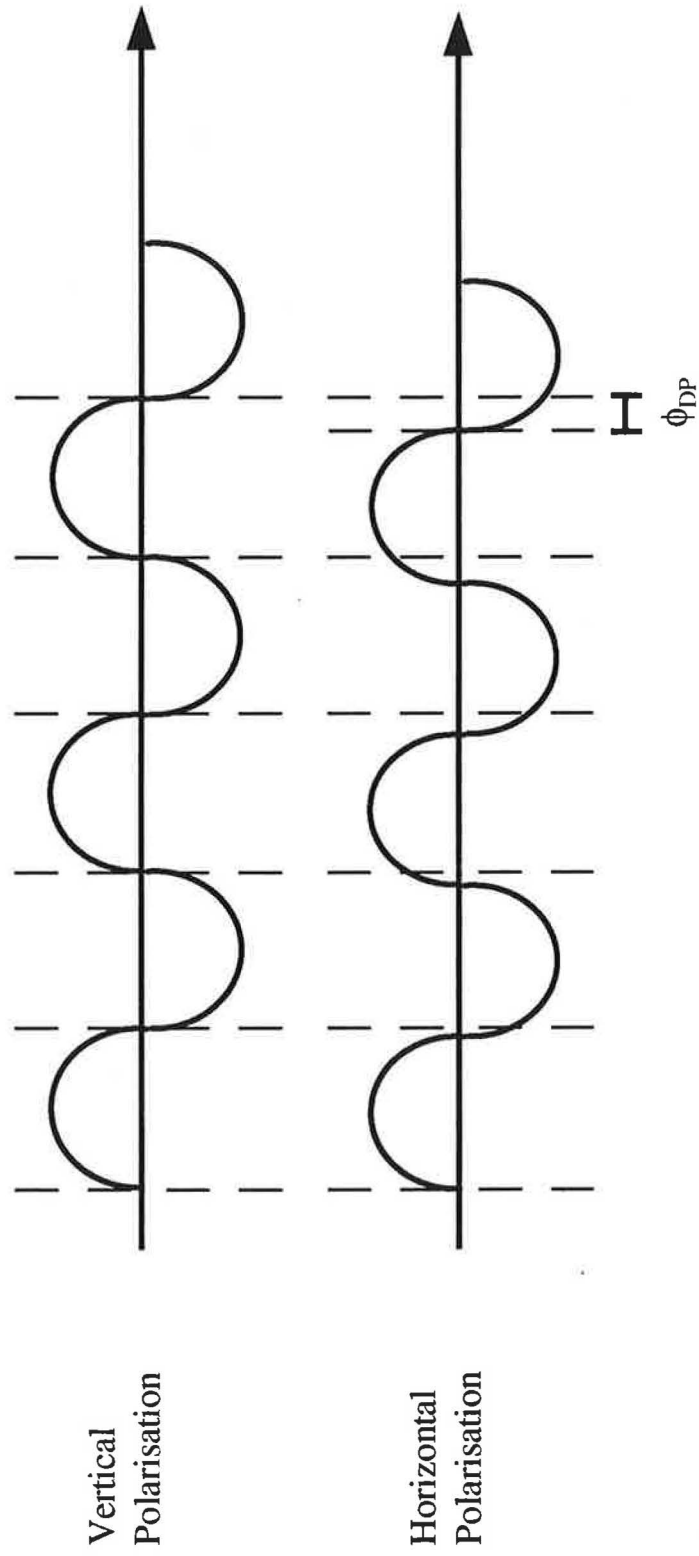


Figure 4: Differential Propagation Phase Shift



better than 0.5 dB, a mechanical switch would be used. The realisation of a practical system is discussed in the next section.

### 3.1 Polariser Assembly

The key to the radar is the polariser assembly (figure 5), located at the focus of the 25 m dish, which embodies the feed, hybrid junction polariser, transmit polarisation switch, transmit-receive duplexer, receiver input stage protection, and optical sensors to synchronise the transmitter to the transmit polarisation switch.

Each pulse from the magnetron transmitter initially feeds an E-plane T junction. The two output waveguides from the junction contain a short air-gap occupied by a motor-driven rotary metal disc, the speed of which and hence the radar pulse repetition frequency (PRF), is governed by a variable frequency power supply. The disc has sectors cut out to produce a set of vanes, which are arranged so that when one waveguide port is open, the other is short-circuited, and vice versa. The switch assembly is symmetrical, and the lengths of the output waveguides from the T junction are chosen such that reflected power from the short circuited arm adds in-phase with that transmitted through the open arm. Input matching to the T junction is accomplished with an iris plate. Power leakage at the waveguide/disc air-gap is minimised using choke flanges. As the disc rotates, the transmitter power is switched alternately between the two output ports which are, in turn, connected to port 3 of a pair of low-loss, high power waveguide circulators. These act as transmit-receive duplexers: port 1 of each circulator connects to a hybrid junction polariser input (H or V polarisation), while port 2 connects to a receiver input via a TR-cell and varactor limiter. The two latter devices provide receiver protection against the leakage of the transmit pulse via the circulator, an important function because with a transmitted peak power of 560 kW, the leakage is of the order of 5 kW.

The hybrid junction polariser, based on a 1940's design by Ragan<sup>5</sup>, contains four rectangular waveguide ports, two of which are terminated in short circuits. By choosing the correct phase shifts from the reference plane to the shorts, it is possible to generate orthogonal linear polarisations in the output circular waveguide leading to the feed. In this case, horizontal and vertical polarisations are chosen, each produced by exciting one of the two remaining rectangular waveguide ports. As a passive, reciprocal network, the polariser functions identically in both transmit and receive modes. Finally, a scalar feed is used to illuminate the dish because of the excellent matching of polar-diagrams in the horizontal and vertical planes.

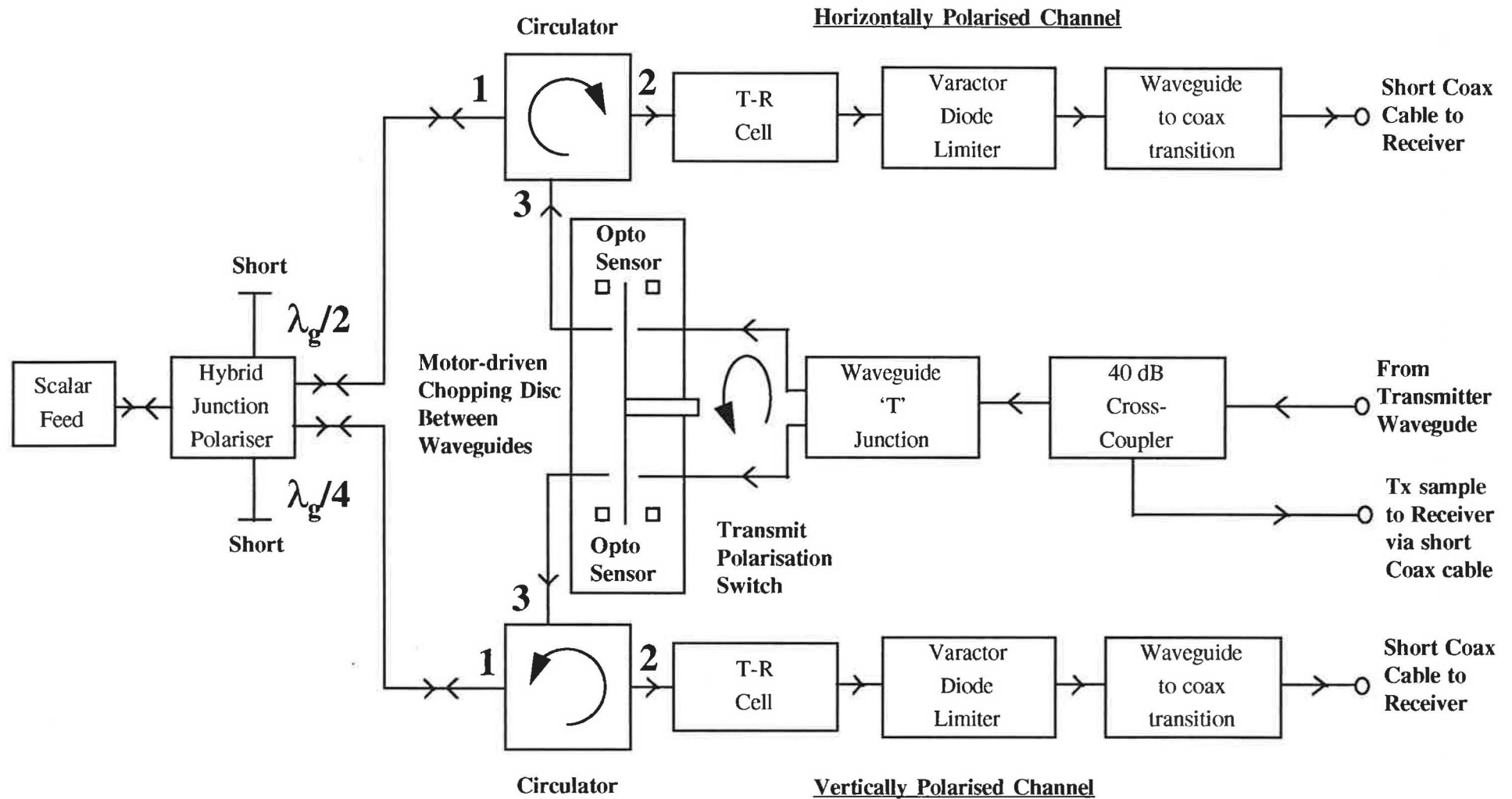


Figure 5: Polariser Assembly

Because of the mode of operation of the transmit switch, it is important to synchronise the firing of the transmitter with the correct positioning of the rotating disc relative to the waveguide ports. The transmitted polarisation state must also be known. This information is provided by optoelectronic sensors consisting of pairs of infrared LED's and photo transistors placed on opposite sides of the disc, the optical path being completed by small holes through the disc at the appropriate locations. The photo transistors drive signal conditioning circuitry, and two digital outputs are produced to drive the transmitter control logic and the data acquisition electronics.

### 3.2 Dual-Channel receiver

The primary function of the dual channel receiver (figure 6), also located at the focus of the 25 m dish, is to allow simultaneous measurements of co-polar and cross-polar reflectivities. It comprises the receive polarisation switch, dual down converter chain, transmit pulse sampler and down converter, plus an amplitude calibration unit.

The receive polarisation switch takes its two inputs from the horizontal (H) and vertical (V) receive ports of the circulators in the polariser assembly, via the receiver protection components and short, low-loss coaxial interconnecting cables. The two outputs of the PIN diode transfer switch are connected to the co-polar and crosspolar receiver inputs. The control input of the switch is driven by a square wave derived from the transmit polarisation state output from the polariser optoelectronic sensors. The commutating action of the switch is such that for input signals of H and V, two outputs are produced. One output (CO) is always co-polar with the transmitted polarisation state, while the other output (CROSS) is always cross-polarised. The insertion loss due to the receive switch is 1 dB.

The outputs of the receive switch drive the dual down converter chain, two identical receivers sharing a common local oscillator. Each receiver comprises a Ga As FET low noise amplifier preceded by a directional coupler for calibration signal injection. The output from the LNA passes through an isolator to ensure correct termination of the LNA output over its full operating bandwidth, a bandpass filter to provide image rejection and an adjustable attenuator to set the overall front end gain. Finally, it is applied to a mixer whose 30 MHz output is bandpass filtered and amplified before being fed through approximately 200 m of coaxial cable to the I.F. processor in the Radar Control Room. The overall receiver gain and noise figure are 45 dB and 4 dB, respectively, including losses in the receive switch. The dynamic range is around 90 dB in a 4 MHz bandwidth.

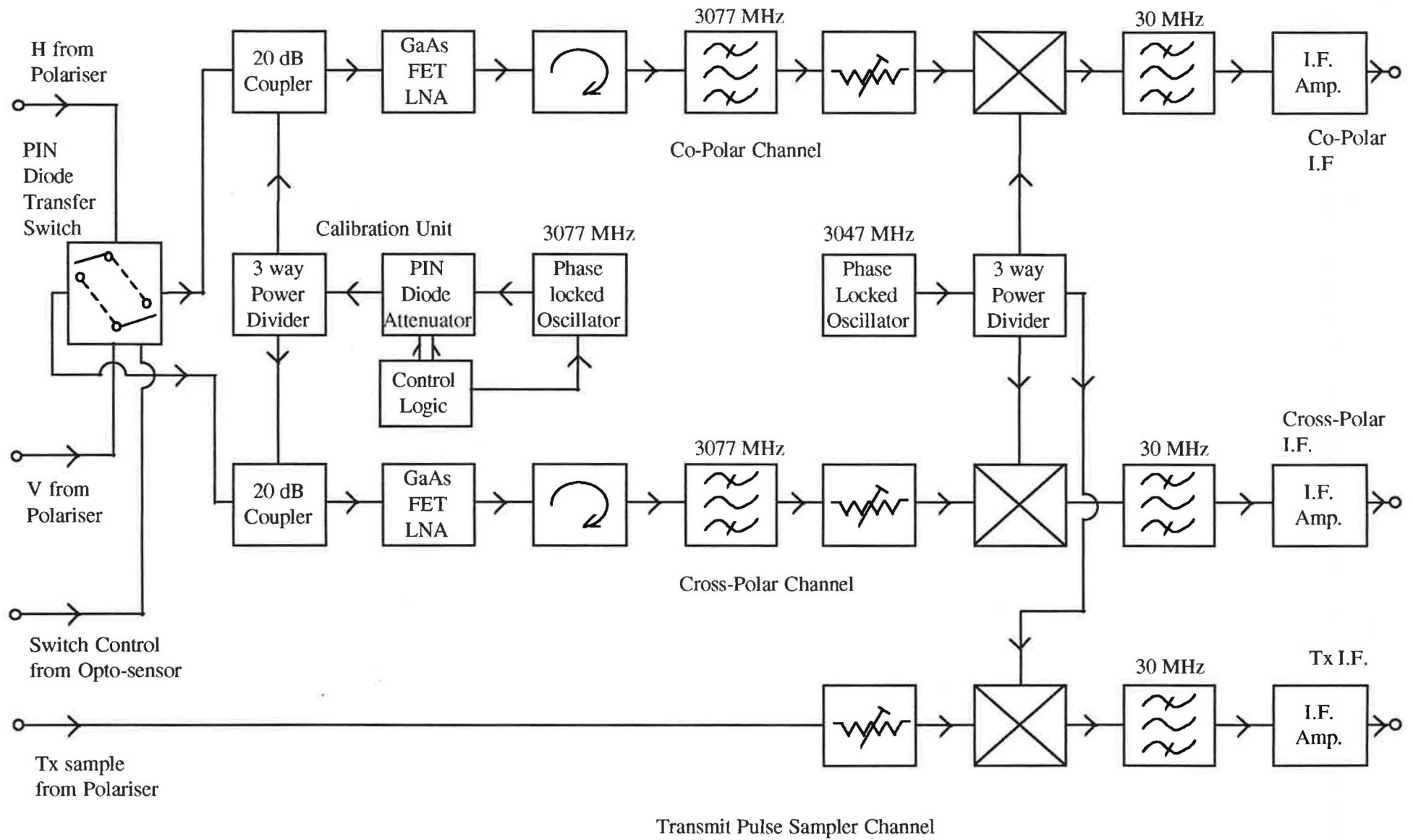


Figure 6: Dual Channel Receiver

The transmit pulse sampling system is necessary in order to make Doppler and phase measurements with the essentially incoherent magnetron transmitter. The starting phase of each transmitted pulse is random. However, if both the phase of the transmitted pulse and that of the return from the radar target are measured, then the phase due to the target alone may be determined by subtraction of the phase angles. To measure the phase of the transmitted pulse, a waveguide cross-coupler is used to obtain an attenuated sample of the signal in the waveguide run between the transmitter and the polariser. After further attenuation, this drives a mixer fed with the same local oscillator that feeds the dual down converter chain via a three way power divider. The local oscillator itself is phase locked to an oven controlled crystal reference. The 30 MHz output from the mixer is bandpass filtered and amplified before being fed via another 200 m coaxial cable to the control room.

The built-in calibration unit is used to routinely characterise the performance of the receiver front end and I.F. processor over a large dynamic range. Although experience has shown that the gain stability of the complete system is good, the calibrator enables changes in absolute gain (which would effect Z estimates) and differential gain between the two down converter chains (which would effect cross-polar estimates) to be measured. It consists of a crystal controlled oscillator at the transmitter frequency feeding an 8 bit PIN diode attenuator, the output from which is introduced into the receiver inputs via a three way power divider, two ports of which feed the coupled ports of the 20 dB directional couplers preceding the LNA's. The third port of the three way power divider is used to periodically check the injected power levels. When a calibration is called for, the control logic steps the PIN attenuator in 0.25 dB increments over a 64 dB dynamic range, enabling the full transfer characteristic of the front end, I.F. system and data acquisition electronics to be determined.

### 3.3 I.F. Processor

The I.F. processor (figure 7) accepts the three 30 MHz inputs from the dual channel receiver, namely the co-polar I.F., cross-polar I.F. and the transmitter I.F. sample (CO I.F., CROSS I.F. and TX I.F. respectively), and produces video outputs of co-and crosspolar magnitude and phase. For clarity, it is convenient to divide the processor into two parts: that dealing with phase and that dealing with magnitude, although in the actual hardware implementation, the system is divided into one unit for the co-polar I.F. and another for the cross-polar I.F.

#### 3.3.1 Magnitude (Z) processing:

In order to make use of the large dynamic range of the front end system, the I.F. processor needs to operate over an even larger range of magnitude. Logarithmic amplifiers are used to

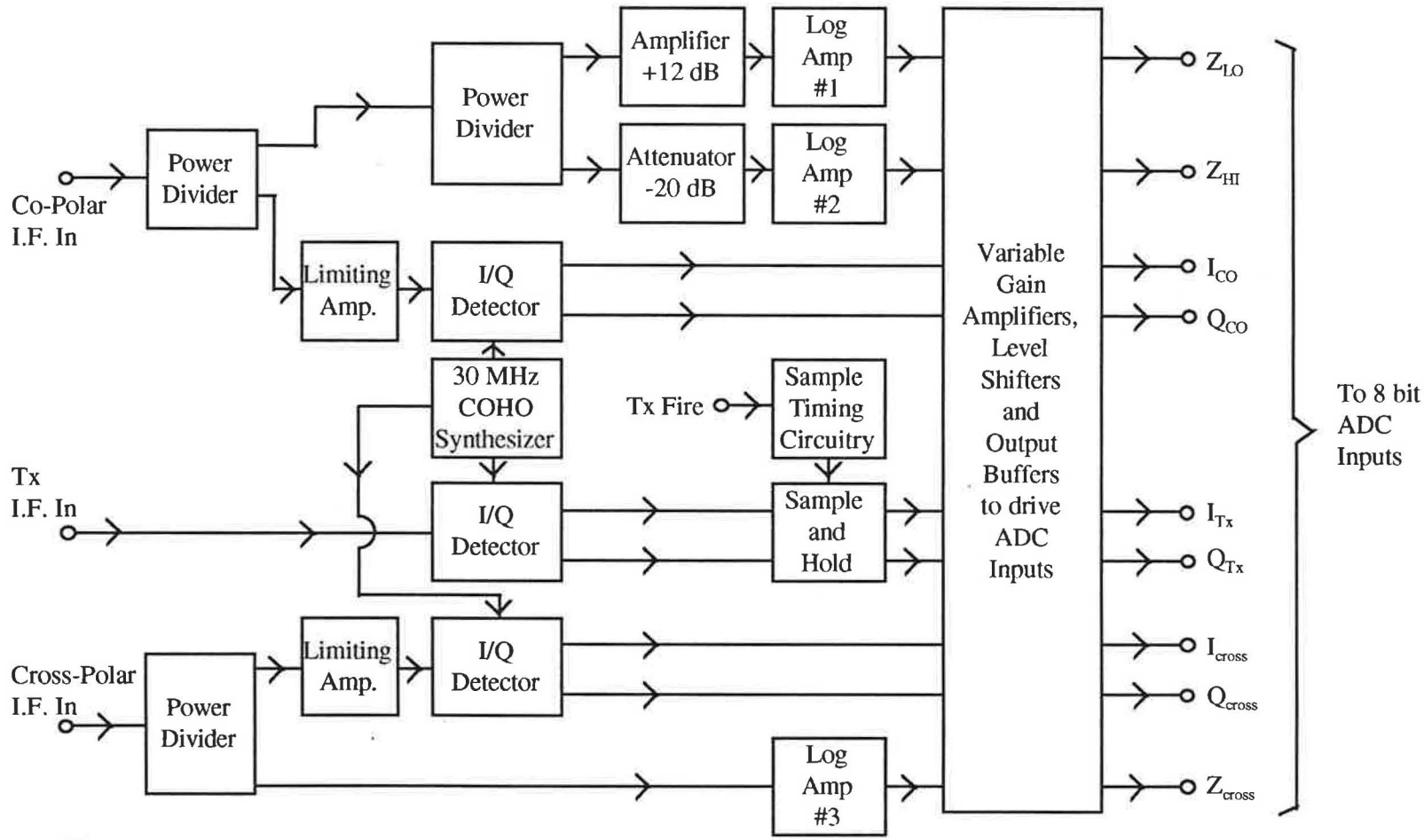


Figure 7: I.F. Processor

process the I.F. signals, but conventional units only exhibit good log-linearity over a 60-70 dB range. To cope with the 90 dB range requires, for the co-polar channel, a pair of log amplifiers with overlapping transfer characteristics. If the front end dynamic range is correctly mapped into that of the I.F. processor by suitable choice of the system gain, then the optimum overall dynamic range is obtained. The video outputs of the two log amplifiers, designated  $Z_{HI}$  and  $Z_{LO}$ , are digitised to 8 bit precision and combined in digital hardware to produce a 9 bit representation of  $Z_H$  in a 96 dB range with 0.25 dB resolution.

The required dynamic range for the cross-polar channel is rather less than for the co-polar due to the limited extent to which typical meteorological targets depolarise. An 80 dB range is satisfactory, and this is achieved by a single log-amplifier with acceptable log linearity. The cross-polar video,  $Z_{CROSS}$ , is digitised to 8 bit precision with 0.5 dB resolution. All ADC's operate at 2 MHz, and are buffered via FIFO's prior to signal processing.

### 3.3.2 Phase ( $\phi$ ) processing

The phase processing electronics consists of three I/Q detectors (figure 8) for co-polar, cross-polar and transmitter phase determination, respectively. The co- and cross-polar I/Q detectors are driven by I.F. limiting amplifiers of low AM/PM conversion, while the transmitter phase detector is driven directly by the signal from the front end unit. The I/Q detectors themselves are constructed from an array of lowpass filters, power dividers, phase shifters and double-balanced mixers, as shown in the figure. Coherent local oscillator (COHO) injection for the mixers is provided by a programmable synthesizer. The amplitude and phase balance and tracking with respect to I.F. variations was carefully checked with a vector voltmeter. Very good performance was achieved using low cost components.

The I and Q outputs from the co-polar phase detectors are continuously digitised at 2 MHz and processed by the DSP card to yield a characteristic angle for each range gate. The transmitter phase is determined once per pulse by processing the I and Q outputs from a dual sample-and-hold gate which is enabled at a well defined time during the transmit pulse. For each transmit pulse, the transmitter phase angle is subtracted from the receive phase angle at each gate, to yield the required target phase estimates, using the signal processor described in section 4.

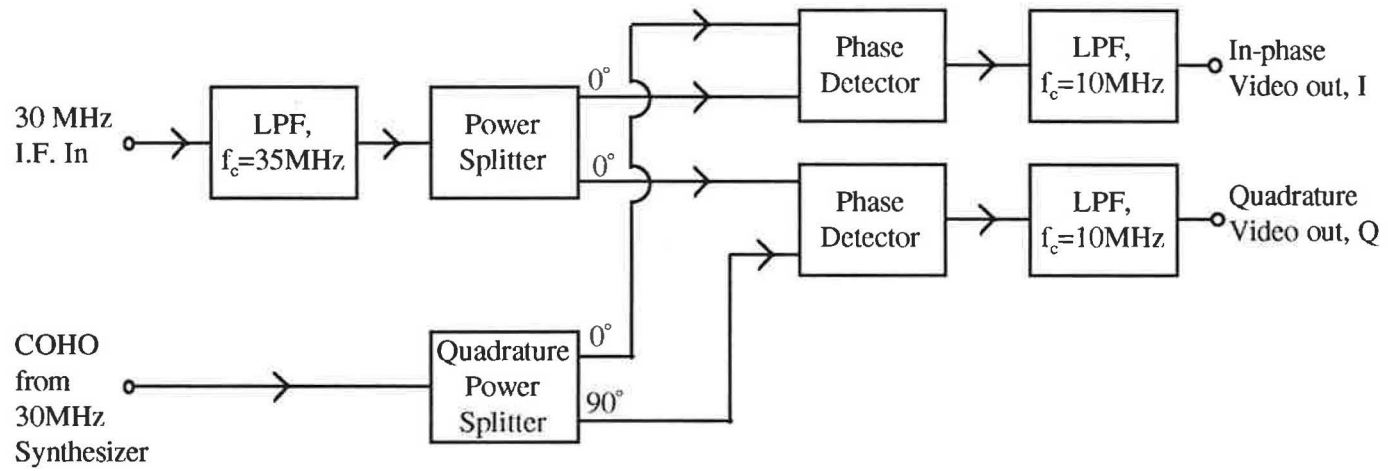


Figure 8: I/Q Detectors



## 4. Signal Processing

### 4.1 Theory of statistical sampling of Reflectivity and Differential Reflectivity

Because the precipitation echo measured by a meteorological radar comes from an ensemble of individual scatterers which are randomly distributed within a given resolution volume, it fluctuates randomly. It is therefore necessary to average the received power,  $P_r$ , to obtain a reliable estimate of the mean value. In doing this, some assumptions are made : (i) the fluctuating signal is ergodic so that both ensemble and time averaging can be used; and (ii) many small scatterers are randomly distributed in a resolution volume whose dimensions are much larger in size than the radar wavelength, so that the phase of the composite return signal is uniformly distributed between 0 and  $2\pi$ , and the amplitude is Rayleigh distributed.

It follows from assumption (ii) that the instantaneous return power is exponentially distributed and that its probability density function has a standard deviation equal to the mean value. A single measurement of  $P_r$  therefore suffers from a large error and, in order to reduce the estimation error, it is necessary to average many statistically independent samples. The averaging is performed after detection of the IF signal. In the case of the Chilbolton radar, logarithmic detection is used in order to increase the dynamic range. However, averaging in the log domain introduces a systematic bias, and the technique employed on the Chilbolton radar is to convert each sampled log value to a linear power before averaging.

Providing the number of independent samples,  $N$ , is greater than about 10, the fractional standard error of the mean power, and hence of reflectivity  $Z$ , in dB units is :

$$\sigma_z = 10 \log_{10} \left[ 1 + \frac{1}{\sqrt{N}} \right] \quad [3]$$

Although it is advantageous to have a large number of independent samples, it is nevertheless important to ensure that the micro physics does not change during the time sequence of samples. The time interval between successive pulses of the same polarisation is 3.2 ms, compared with a typical rain decorrelation time of 10 ms at S-band, so not all pulses are decorrelated. Normally, the Radar averages 64 H and 64 V pulses, which takes approximately 210 ms, and additional range averaging over groups of 4 gates (each of 75 m length) is used to further increase the number of independent samples so that a standard fractional error of 0.75 dB for  $Z$  measurements is readily obtained.

For  $Z_{dr}$ , the estimates need to be measured to better than 0.2 dB accuracy. To achieve this standard deviation, one would normally need to process 1000 independent samples of  $Z_H$  and

$Z_V$ . However, another approach is to make use of the high correlation which consecutive samples of  $Z_H$  and  $Z_V$  have when taken at sufficiently small time intervals. It turns out that in this case an optimum estimator of differential reflectivity<sup>6</sup> can be obtained using:

$$\overline{Z_{dr}} = \frac{1}{M} \sum_{i=1}^M (Z_{H_i} - Z_{V_i}) \quad [4]$$

This leads to an accuracy of 0.2 dB for 64 pairs of H and V samples.

Apart from minimising the standard deviation of  $Z_{dr}$ , the estimate must also be calibrated to eliminate systematic bias errors. For the Chilbolton radar, this is often done with measurements in drizzle which is expected to have spherical raindrops. Such calibrations are performed for typical angles of elevation used during normal operations, and also for high elevation angles when the raindrops would appear spherical whether large or small. This enables  $Z_{dr}$  to be measured with a systematic error of less than  $\pm 0.1$ dB.

#### 4.2 Doppler velocity and differential phase measurements

Whilst polarisation diversity allows the precipitation structure to be determined with better accuracy, information on dynamics can only be gained from phase measurements. Doppler radars operate on the principle that moving scatterers produce a frequency shift, the mean of which can be determined from the time variation of the phase of the pulse-to-pulse back scatter signal.

If we consider a single target - e.g. a raindrop - moving with a velocity component of magnitude  $V$  towards the radar, this will produce a Doppler frequency shift,  $\Delta f$ , given by :

$$\Delta f = \frac{2V}{\lambda} \quad [5]$$

$\lambda$  being the radar wavelength. In terms of phase, this equates to :

$$\frac{d\phi}{dt} = \frac{4\pi}{\lambda} V \quad [6]$$

where the left hand term represents the rate of change of the back scatter phase. For an ensemble of scatterers with varying drop sizes, each with its own velocity, a Doppler radar will detect a spectrum of frequencies corresponding to the velocity spectrum of the individual scatterers. The upper and lower limits of the Doppler spectrum are determined by the Nyquist

constraint that at least two samples per wavelength are required to measure a frequency unambiguously. This so called Nyquist velocity depends on the pulse repetition frequency which, for the case of Chilbolton radar, is 305 Hz per polarisation. At 3 GHz, this results in velocity limits of -7.5 and +7.5 m/s.

There are two basic signal processing approaches adopted to deduce the characteristics of the velocity spectrum : (i) frequency domain method using power spectrum and (ii) time domain method which uses auto-correlation function. In the latter category, one particular technique that was developed in the 1970's is the pulse-pair estimator which was soon established as the most efficient method for real-time applications. With this technique, the mean velocity is given by :

$$\hat{v} = -\left(\frac{\lambda}{4\pi T_s}\right) \arg(\hat{R}_a \cdot \hat{R}_b) \quad [7]$$

where  $T_s$  represents the pulse repetition time,  $\arg$  is the arctangent of the complex quantity with the brackets, and  $R_a$  and  $R_b$  are the pulse pair covariance between the complex signals in the H (horizontal) and V (vertical) channels, given by :

$$\hat{R}_a(T_s) = \frac{1}{N} \sum_{i=0}^{N-1} V_{2i}^* \cdot H_{2i+1} \quad [8]$$

$$\hat{R}_b(T_s) = \frac{1}{N} \sum_{i=0}^{N-1} H_{2i+1}^* \cdot V_{2i} \quad [9]$$

Note that H and V in these equations are expressed in terms of the measured I and Q of the respective channels, as complex quantities of the form  $I + jQ$ . There are several advantages of using the pulse-pair technique. One is that it can be easily implemented in software or hardware for a substantial number of gates. Secondly, equations (8) and (9) also enable the differential phase shift between H and V signals,  $\phi_{dp}$ , to be determined in a straightforward manner. As mentioned earlier, this quantity is a measure of the extra phase delay suffered by a horizontally polarised wave as it passes, for example, through oblate raindrops, compared to the phase of the vertically polarised wave<sup>7</sup>, see figure 4. A simple estimator of  $\hat{\phi}_{dp}$  which uses  $R_a$  and  $R_b$  is

$$\hat{\phi}_{dp} = \frac{1}{2} \arg(\hat{R}_a \cdot \hat{R}_b^*) \quad [10]$$

The two quantities  $arg(R_a)$  and  $arg(R_b)$  contain contributions from Doppler velocity as well as differential phase. By adding the two (as in equation [7]), we effectively cancel the  $\phi_{dp}$  effects. Conversely, by subtracting the two, we cancel the Doppler effects (as in equation [10]). Hence, by evaluating the two covariances, we can efficiently implement the Doppler and  $\phi_{dp}$  algorithms.

#### 4.3 Implementation of signal processing and timing

The IF hardware is interfaced to two digital signal processing (DSP) cards, each of which is resident within a PC (figure 9). The interface is a high speed data acquisition system designed and built specifically for the Chilbolton radar. It consists of two Controller cards and 4 ADC cards, each of which holds 2 X 8 bit 2 MHz ADCs, with associated 2048 byte FIFO memories. The Controller cards use timing signals from the radar system to perform three major tasks :

- (i) wait a predetermined time before initiating sampling
- (ii) determine the sampling rate
- (iii) store a pre-set number of samples from the ADCs in the FIFOs.

The counting and timing functions are all controlled by two 3-channel counter-timers (82C54) coupled to the I/O bus of the PC computers. This enables a high-level language to be used to initiate data collection. Once the 82C54 is programmed, the system cycles indefinitely, until reset.

The reflectivity processing system (figure 9, top) produces  $Z_H$ ,  $Z_{dr}$  and also a cross-polar signature,  $L_{dr}$ , defined as:

$$L_{dr} = 10 \log_{10}(Z_{H,V}/Z_H) \quad [11]$$

where  $Z_{H,V}$  is the signal received in the horizontal polarisation channel from a vertically polarised transmission. A separate system processes the phase measurements (figure 9, bottom). For the former, the output from the interface unit consists of 1 channel for the co-polar and 1 channel for the cross polar signals. Digitised data are transferred via a high speed "hyperbus" link which looks like a fixed memory location on the DSP card. Hence, by issuing simple memory-read commands from the DSP card, the data from FIFO buffers are accessed.

Each signal processing card contains two Motorola DSP chips, both of which have various types of internal memory (i.e. on-chip RAM, SRAM and DRAM), some of which is shared memory. The data from the FIFOs is piped to one of the processors which organises and

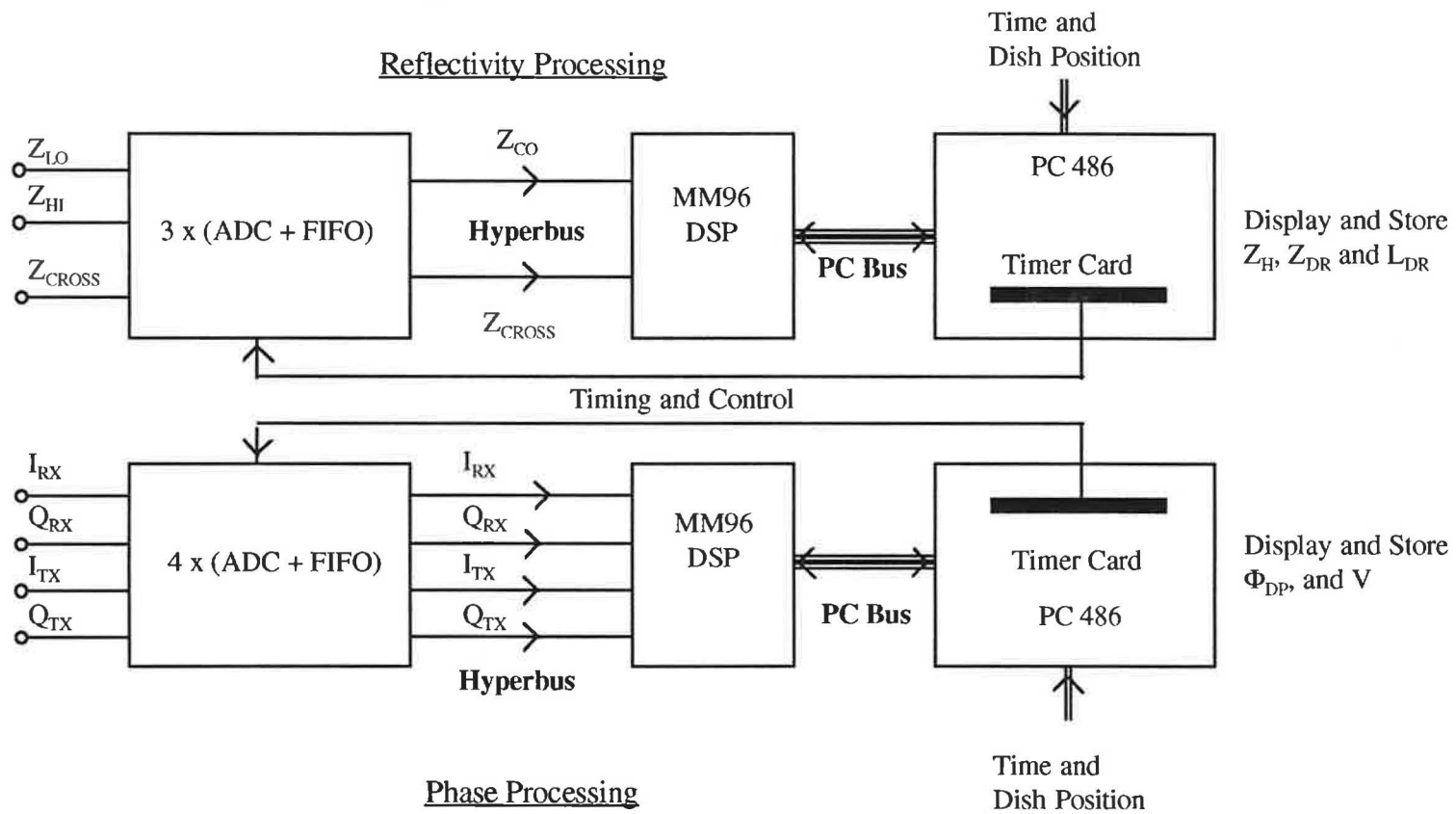


Figure 9: Signal Processor

accumulates the pulse-to-pulse data for the amplitude system. A lookup table containing linear equivalents of all log power values is stored in fast on-chip RAM for linear power averaging. Once 64 pairs of pulses have been acquired, the first processor sets a flag for the second processor to indicate that accumulated data are ready in shared memory for final processing. This consists of range averaging and the conversion of  $Z_H$ ,  $Z_{dr}$  and  $L_{dr}$  to dB units.

The code on the DSP is written in assembler language down-loaded from the host PC. The PC itself is programmed in "C" and is able to communicate with the timer card (see above) to control the ADC operations. Processed data from the DSP are available through a 32-bit full duplex parallel port which is connected directly to the PC data bus. The PC also accesses messages from the antenna control computer through a serial port, giving information on dish position and time, both of which are stored as record labelling for every 64 pulse data average. The PC also provides a real-time display of the three processed parameters.

For the phase system, the DSP needs to perform substantially more operations. As seen in section 4.2, the processing is essentially composed of complex multiplications (i.e. evaluation of  $R_a$  and  $R_b$  in equations [7] and [8]). Before this stage, however, we need to evaluate the complex signals H and V from their respective I and Q measured for the received signal. This first requires the subtraction of the transmitter phase, because the Tx signal is generated with a random phase. The phase subtraction involves more complex multiplications, and this has to be done for each pulse. The subtractions are performed on one of the DSP chips, which, when complete, sets a 'ready' flag for the other processor to perform operations to evaluate the running sums in equations [7] and [8]. At the end of 64 H and V pulses, the resulting values of  $R_a$  and  $R_b$  are used to determine Doppler velocity and differential phase which are then transferred to the PC for storage and display.

#### 4.4 Data logging programme

The data logging programme receives data in units of 'rays', that is, at the end of every 64 pairs of H and V pulses. The data are sent over the 8 MHz PC bus indefinitely every 0.21 seconds approximately. The programme must receive each ray to keep in synchronisation even if the data are not used, thus the processing time on the PC must not exceed the reception rate.

Once a ray has been received, the dish position is checked by monitoring the serial port 'COM 1' (see Figure 10). Further action is then dependent upon the asynchronous information received via serial port 'COM 2', which is specified by the user on the radar control computer. The display and storage of the data are only performed when the dish position is within the user-

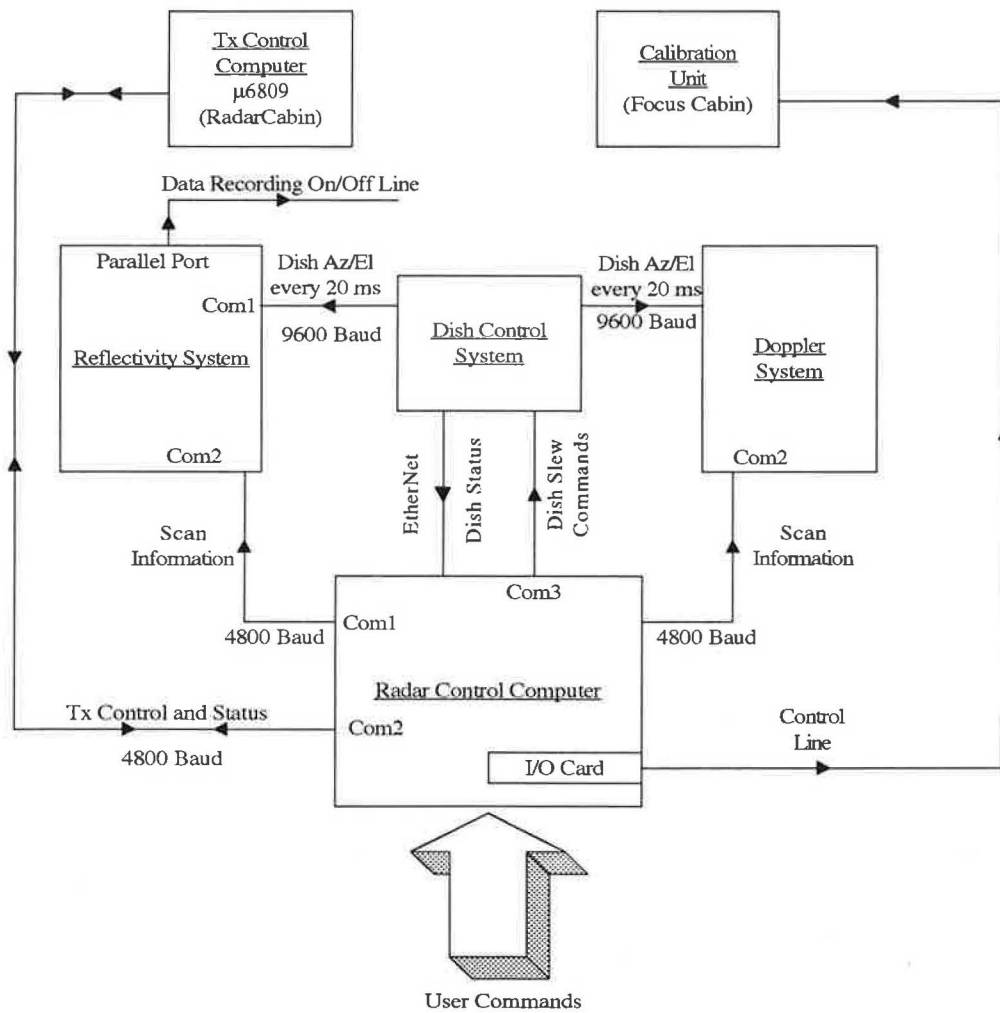


Figure 10: An overall view of the Radar Control and Data Acquisition System

defined limits. The data are then range normalised, calibrated and thresholded before being stored.

The maximum work load that is put on the programme is when the ray is to be displayed and stored on disk, which must be accomplished before the next ray is received. The processed data are then written to RAM disk, since the PC internal hard disk is not sufficiently fast to keep up with the data rate. At the end of the data gathering session, the contents of the RAM disk are copied to more permanent media.

The code used by the data logging computers was written in Microsoft C version 6 so that it would be compatible with the software library provided to interface with the signal processing system. However, because this version does not support the 1024 by 768 by 256 colour colour modes required for a meaningful display resolution, a compatible graphics package, "Meta-graphics", produced by Meta-windows was used. Both of these products were also compatible with the PHARLAP 286 dos extender which meant that there was no restriction to running the programme in the normal 640 Kb dos memory limit. At the time when the project was initiated, Microsoft C was still a 16 bit compiler, so a 386 dos extender could not be used, even if a compatible product had been available. The PC's presently in use are 33 MHz 486 machines.

#### 4.5 The dish control programme

The dish control programme is a menu driven system written in Borland C++ version 3.1. With this system, the user can specify a number of characteristics including : - scan type (Range height indicator for vertical scans through rain, Plan position indicator for horizontal scans, slant plane or fixed bearing), minimum distance and range over which to process the data received, control of the transmitter and the monitoring of its power level, control of the radar calibration unit, range gate separation and spacing for both systems and an ON/OFF toggle for data record mode. The programme then communicates the necessary information to the data logging system via the serial port Com 1. This interprets the user commands regarding the forth coming scan. The programme also communicates with the dish control system via the serial port Com 3 and an ethernet link; the serial port is used to send commands regarding antenna slews and the ethernet link is used to monitor the dish status. A further serial port, Com 2, is used to communicate with the radar control computer in the radar cabin (see Figure 10) on the 25 m antenna. An I/O card is used to communicate with the radar calibration system.



## 5. Examples and Applications

### 5.1 Primary Products

The most common scanning modes are vertical slices (RHI), which give information about the vertical structure of rain, or constant elevation slices (PPI), which give information about the horizontal structure. The Chilbolton radar can now measure 5 parameters simultaneously, and an example of a PPI scan at 1° elevation is shown in figure 11. An intense area of rain can be seen near the centre azimuth between 20 and 30 km range, with reflectivities approaching 40 dBZ. The  $Z_{dr}$  parameter indicates the presence of large raindrops in part of this area. The cross-polar ( $L_{dr}$ ) parameter shows returns about 30 dB below the co-polar values, indicating that the rain drop's major axes are aligned to within 5 degrees or so of the horizontal plane. Differential phase increases steadily through this rain, from zero degrees at close range, to about 10 degrees at 60 km range. The Doppler velocities are positive (towards the radar) in the bottom right of the scan, increasing steadily towards the top left, with a 'fold' from +7.5 m/s to -7.5 m/s due to the Nyquist constraint mentioned earlier in section 4.2.

An example of a vertical section through the same rain is shown in figure 12. A clear indication, at 2 km, of the height of melting can be seen in all three parameters. Although this is an example of widespread rain, there is a stronger core of rain at 12 km range where rainfall rates exceed 30 mm/h. This core contains significantly larger rain drops than the surrounding weak rain.

### 5.2 Secondary Products and Examples of Applications

The most useful parameters for rainfall rate and microwave attenuation estimation are  $Z$ ,  $Z_{dr}$  and Differential Phase. Because  $Z$  and  $Z_{dr}$  characterise the rain DSD, they can provide reliable estimates of both rainfall rate and microwave attenuation. Accurate estimates of rainfall are of great importance for hydrology applications, such as flood forecasting, river flow control and urban drainage schemes. The Chilbolton radar is being used in all these areas through collaborations with Universities and Meteorological agencies in both the UK and Europe. Of great importance for World Climatology and Global Warming is the use of satellite remote sensing techniques. The efficacy of algorithms to obtain surface rain fall rates from multi-frequency satellite radiometers is currently under scrutiny, using the wide area coverage of the Chilbolton radar to provide 'ground truth' information. With an eye to future satellite radar missions, studies have also been carried out with Japanese scientists to quantify errors that may arise when a satellite radar is used to estimate global rainfall.

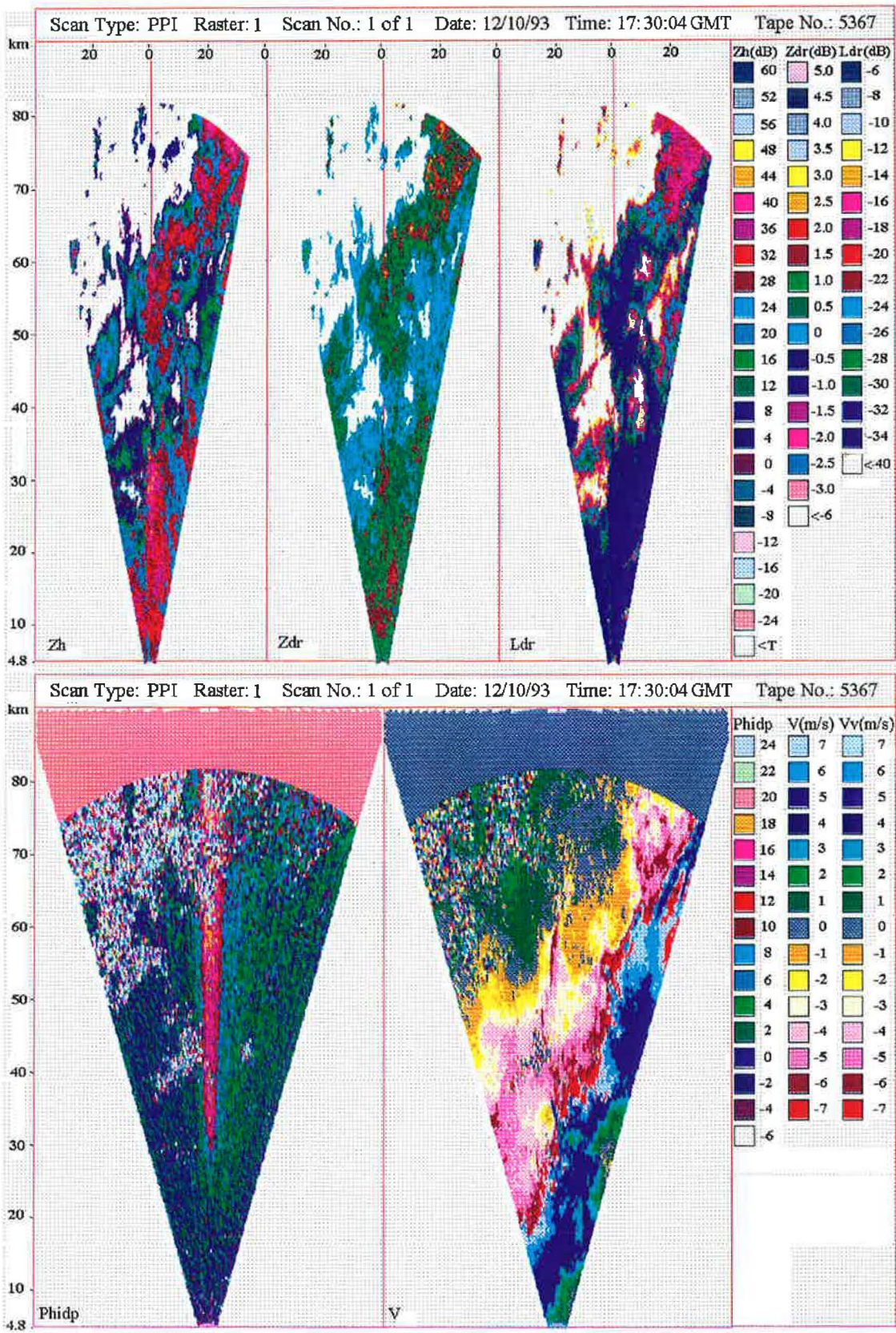


Figure 11: Horizontal scan through rain on 12th October 1993 at 1738 GMT  
 (Top row, left to right, Reflectivity, Differential Reflectivity and Linear Depolarisation Ratio)  
 (Bottom row, left to right, Differential Phase and Doppler Velocity)

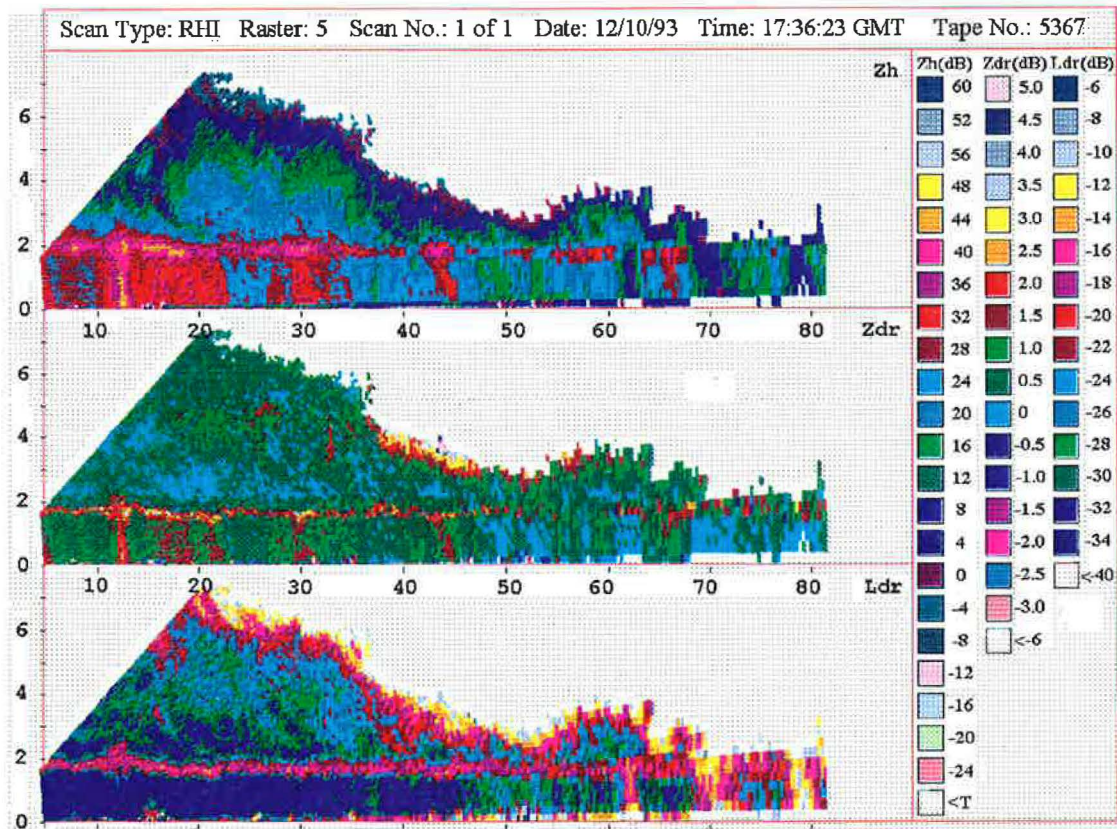


Figure 12 : Vertical section through ice and rain on 12th October 1993 at 1736 GMT.  
 (Top - Reflectivity, Middle - Differential Reflectivity, Bottom - Linear depolarisation ratio)

Another area, this time in the field of meteorology itself, is the characterisation of ice crystals and estimation of their equivalent water content. This study is still in the investigative stage and is being conducted in collaboration with research scientists at National Center for Atmospheric Research at Boulder, Colorado, USA. There have also been several joint campaigns with the C-130 research aircraft belonging to the UK Meteorological Office to study the early stages of convective events, supercooled rain drops, melting process of hail and graupel and the role of ice particles in wet growth.

In the field of radio communications, the radar has contributed in two main areas. It has been used to quantify rain effects such as attenuation and depolarisation of signals on satellite paths and terrestrial line-of-sight paths. For example, a major programme of work for the radar has been in conjunction with the Olympus satellite, which had propagation beacons at 12.5, 20 and 30 GHz. Radar measurements made along the rain-affected part of the Earth-Space path can be used to estimate microwave attenuation at all three frequencies, simultaneously. An example of these estimates compared with the actual beacon measurements, during an intense event in July 1992, is shown in figure 13. The small differences between the radar estimates and the direct measurements can be easily accounted for by gaseous (oxygen and water vapour) attenuation which the radar cannot quantify. The second application in the communications area is the evaluation of interference caused by rain scatter between systems sharing the same frequency. Under the framework of a European collaborative project, data from the Chilbolton radar were used to simulate such interference and help develop improved models for interference prediction.

## **6. Concluding Remarks**

The last decade has seen great strides forward in the methods of sensing and understanding of rain systems. The UK has been at the forefront of these developments and the Chilbolton radar has played a major part in this, acting as a state-of-the-art tool for University and other groups in the fields of radiowave propagation, cloud physics and meteorology. The future looks equally exciting, with plans (some already fulfilled) to install higher frequency radars on the same antenna, which will be capable of sensing smaller cloud particles, simultaneously with the 3 GHz rain measurements.

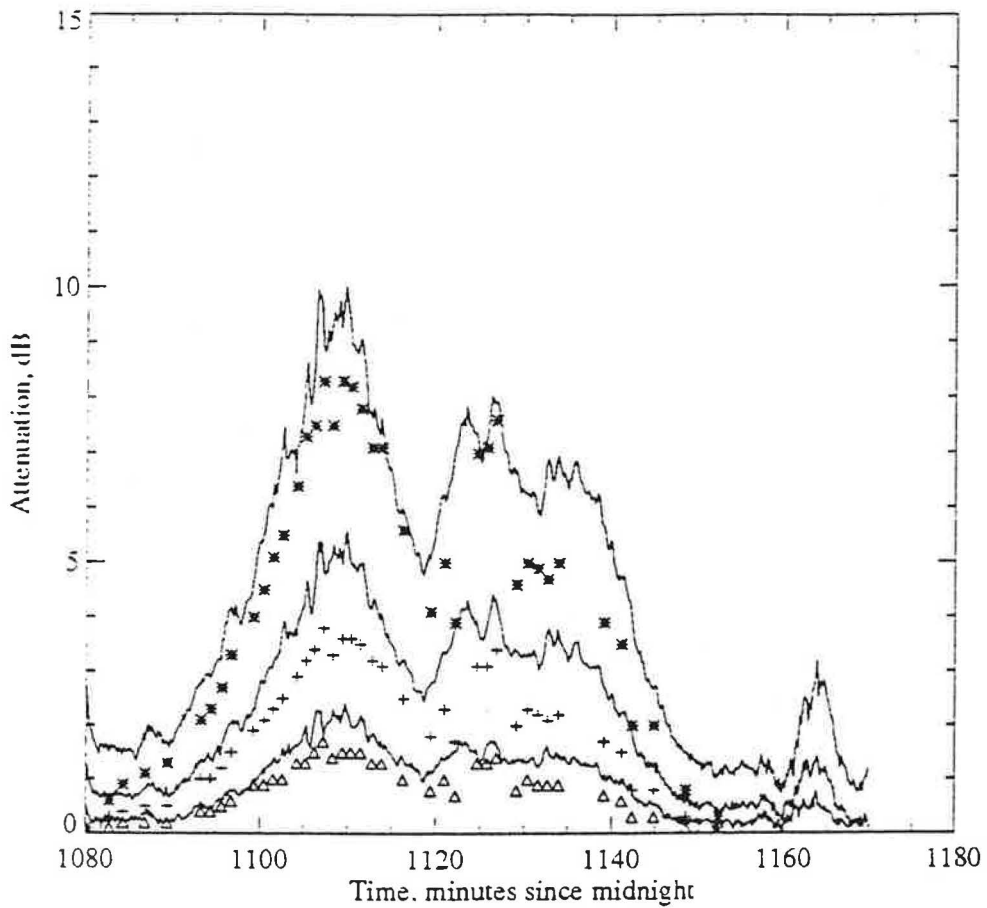


Figure 13: Attenuation at 12.5, 20 and 30 GHz for 20th July event.  
 Beacon measurements at 3 frequencies ———  
 Radar 12.5 GHz  $\Delta \Delta \Delta$  20 GHz  $+++$  30 GHz  $***$

## 7. Acknowledgements

Many individuals have contributed to the development of the Chilbolton radar since the early 1970s, but the authors would like to acknowledge the contributions of Martin Hall and Steve Cherry who initiated the project, and Anthony Illingworth, formerly of UMIST, but now at Reading University, whose team of enthusiastic scientists, funded by NERC and SERC, have provided a steady stream of new ideas and scientific expertise. Finally, the role of the Radiocommunications Agency in providing financial support for the propagation portion of the radar programme is gratefully acknowledged.

## 8. References

1. Seliga, T.A. and Bringi, V.N., 1976: Potential use of radar differential reflectivity measurements at orthogonal polarisations for measuring precipitation. *J. Appl. Meteor.*, **15**, 69-76.
2. Hall, M.P.M, Goddard, J.W F. and Cherry, S.M., 1984: Identification of hydrometeors and other targets by dual-polarisation radar. *Radio Sci.*, **19**, 132-140.
3. Illingworth, A.J., Goddard, J.W.F. and Cherry, S.M., 1986: Detection of hail by dual-polarisation radar, *Nature*, **320**, 431-433.
4. Goddard, J.W.F, Tan, J and Thurai, M., 1994: A technique for the calibration of meteorological radars using differential phase, *Electronics Lett* (*in press*).
5. Ragan, G.L. 1948: Microwave Transmission Circuits, pp375-377, 533-534, McGraw Hill.
6. Bringi, V.N., Seliga, T.A. and Cherry, S.M., 1983: Statistical properties of the dual polarization differential reflectivity ( $Z_{DR}$ ) radar signal. *IEEE Trans. Geosci. Remote Sens.*, **GE-21**, 215-220.
7. Seliga, T.A. and Bringi, V.N., 1978: Differential Reflectivity and Differential Phase Shift: Applications in Radar Meteorology, *Radio Sci.*, **13**, 271-275.

